J. Webster (ed.), *Wiley Encyclopedia of Electrical and Electronics Engineering*

TRANSFORMERS, LIQUID-FILLED

Transformers (1) consist of two or more coupled windings (typically one high-voltage, low-current winding and one low-voltage, high-current winding) surrounding an iron core, which increases and directs the mutually linked flux for a given alternating current (*ac*) excitation of the windings. Liquid-filled transformers are important components of a power system consisting of generation, transmission, distribution, and electrical loads; such transformers cover a wide apparent power range from 10 kVA to 800 MVA. Transformers permit the change of voltages and currents to match generation of electrical power with consumption, and provide galvanic isolation of electrical networks. There are single-phase and multiphase (e.g., three-phase) transformers. An example of the former type is the pole transformer of a distribution system; the latter are power plant, (sub)transmission, and substation transformers (2). Transformers permit the efficient and optimal transmission of power through the above-mentioned functions.

The design concept of a typical liquid-filled, single-phase transformer consists of a primary winding, a secondary winding, a laminated iron core, a solid iron tank, coolant (transformer oil, for example), overcurrent and overload protection equipment, and switches to disconnect the unit from the power system in case of failure. The coolant (3,4,5) permits a greater overload capacity of transformers through intense cooling employing fans and pumps. This can be compared with dry-type transformers, which are only manufactured at small ratings (up to 100 kVA). Liquid-cooled transformers have windings and core submerged in the liquid, which may be mineral oil, silicone fluid, or synthetic fluid materials (e.g., Askarel).

Natural circulation of the liquid due to the heat gradient is used in some of the units. Fins are normally provided to dissipate the heat to the surrounding air, and fans may be employed to facilitate the removal of heat from the transformer cooling liquid. Alternatively, a water jacket with circulating cold water may be inserted inside the transformer housing to cool the liquid. Another method, which does not depend on the natural circulation of the liquid, pumps cooling liquid through the fins and/or radiator. An effective cooling system can increase transformer capacity by 50%. Under these circumstances, a unit with 100% output power capacity may be operated at up to 150% capacity without causing damage to the transformer.

However, synthetic cooling liquids sometimes cause skin irritation, and one must be careful not to become exposed to them. Some types of synthetic oil used in the past years contain polychlorinated biphenyls (*PCB*s), which are suspected to cause cancer.

Mineral oil coolants—unfortunately flammable—are specially prepared and dehydrated; a moisture content of as little as 0.06% reduces the dielectric strength of the mineral oil by about 50%. They are processed to be free of acids, alkali, and sulfur. To ensure good circulation, they have a low viscosity.

Three-phase transformers consist of three single-phase transformers and are more complicated in their construction and analysis than single-phase transformers. Three-phase units may have additional tertiary windings, and laminated iron or copper or aluminum screens between the core and the tank for the reduction of eddy-current losses within the tank.

Figure 1(a,b) illustrate schematic diagrams of single- and three-phase transformers including their primary and secondary terminal voltages and currents, while Fig. 1(c) depicts a commonly used asymmetric three-phase configuration. Phasor quantities are indicated by a tilde, for example, $\tilde{v}_{\mathrm{p}}(t)$.

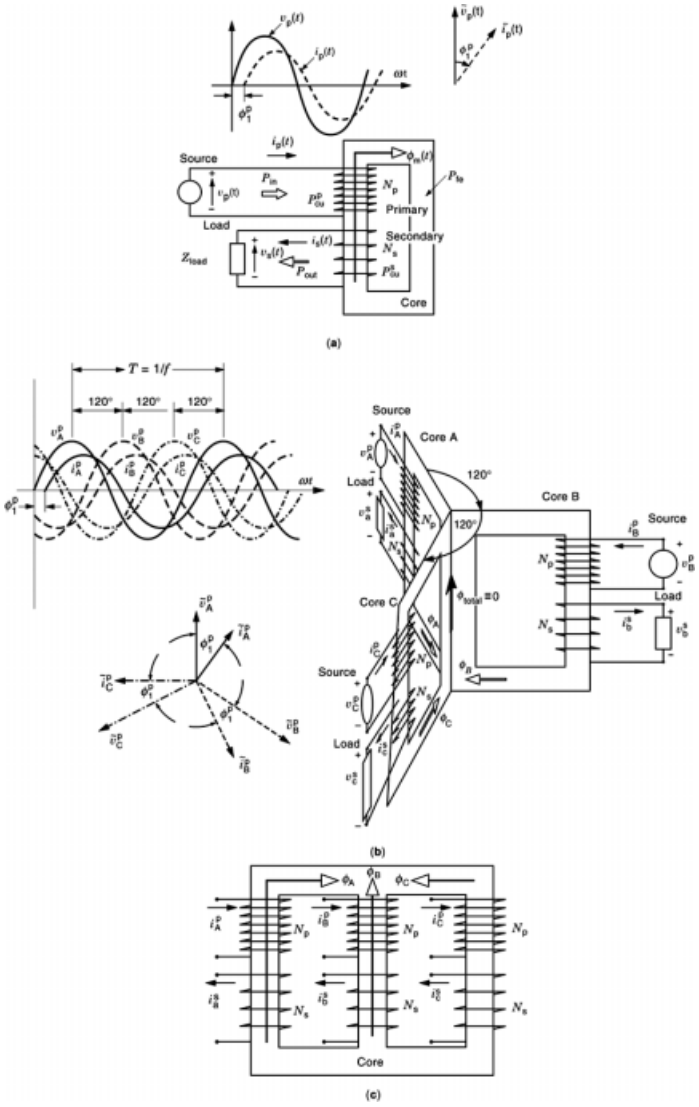

Fig. 1. Single- and three-phase transformer configurations with voltage and current time functions and phasor diagrams; a tilde represents complex quantities or phasors. (a) Single-phase transformer with source and load. Input power P_{in}, output power P_{out}, and losses in windings and core are indicated. (b) Symmetric bank of three single-phase transformers with sources and loads. Voltages and currents are represented in time domain and phasor domain. Fluxes are indicated within core limbs. This configuration illustrates the assembly of a transformer bank. (c) Asymmetric three-phase unit where the limbs are of unequal length.

Transformers need to perform four primary functions: transform ac voltages and currents from one amplitude to another, separate the ground potential of the primary from that of the secondary, act as a filter to block harmonic currents, and efficiently transmit the power from the excited primary to the loaded secondary windings. Here, the principle of power invariance is maintained: the input power must be identical to the output power plus the losses [see Fig. 1(a)].

Although the real power P transmitted is important, the rating of a transformer is expressed in terms of apparent power S. For a single-phase transformer, the rated apparent power is $S_{\text{rat}} = V^{\text{rms}}{}_{\text{rat}} I^{\text{rms}}{}_{\text{rat}}$ measured in voltamperes, where the rated voltage and current are expressed as rms values. Only voltages and currents of fundamental frequency (e.g., $f_1 = 60$ Hz in the United States) are important for energy conversion, and the concepts of apparent (S), real (P), and reactive (Q) powers and the displacement factor cos ϕ_1 (where ϕ_1 is the phase angle between the fundamental components of current and voltage) are employed to discuss the power flow in energy systems. Due to nonlinear loads (6) such as rectifiers and finite-system impedances, the voltages and currents contain harmonics; thus the power factor cos ϕ and the distortion power D become important, taking into account fundamental-frequency (f_1) and harmonic-frequency (f_{h}) voltages and currents.

Ferromagnetic cores of transformers, consisting of oriented (anisotropic) laminated electrical silicon steel, shape and direct the flux. One obtains large maximum magnetic flux densities ($B_{\text{max}} = 1.5$ T to 2.5 T) within cores with low levels of exciting current of the primary; here 1 T = 1 tesla = 10^4 G. It is very important to use laminated electrical steel so that the eddy currents induced within the laminations remain small. Specific loss densities within cores range from 0.1 W/kg to 1 W/kg at a maximum flux density of $B_{\text{max}} = 1$ T and a frequency of $f_1 = 60$ Hz, depending upon the lamination thickness, which ranges from 0.1 mm to 0.4 mm. Oriented and amorphous steel laminations play the most important role in the manufacture of transformers with high efficiencies.

Ferromagnetic materials exhibit hysteresis and saturation effects. At a certain flux density (e.g., $B_{\text{maxsat}} = 1.0$ to 1.5 T) the iron core begins to saturate, and the characteristic curve of flux density B versus magnetic field intensity H becomes nonlinear and valued, exhibiting major and minor B–H trajectories.

The windings of transformers consist mostly of copper or aluminum wire. It is well known that ac signals tend to flow predominantly on the surface of conductors and the current density is less at the center of a thick conductor. To reduce eddy-current development in conductors due to this *skin effect*, thin sheets of copper or aluminum are often used, particularly for the low-voltage, high-current winding(s), which can be either the primary or secondary. To reduce flux leakage, primary and secondary windings are arranged in an interspersed manner, complicating their insulation.

In power systems the demand of power by the consumer is not constant. During a winter day, for example there is peak demand from 9 a.m. to noon and from 7 p.m. to 11 p.m.; reduced-demand periods are from 3 p.m. to 6 p.m. and from 1 a.m. to 6 a.m. This means the utilization of a transformer varies greatly during the day. For this reason, one defines the power (P) efficiency $\eta_{\text{power}} = P_{\text{out}}/P_{\text{in}}$ at the nominal (most efficient) operating point, and also the energy (E) efficiency, which relates to the energy delivered during a load cycle and is defined as $\eta_{\text{energy}} = E_{\text{out}}/E_{\text{in}}$, where $E = \int p\, dt$ is measured in watthours. Usually we have $\eta_{\text{energy}} \leq \eta_{\text{power}}$. While the power efficiency represents a figure of merit, the energy efficiency occurring during a given load cycle is important for a utility because it relates to the efficiency of the transmitted energy and ultimately to the operating cost. Energy efficiency is lower than power efficiency because the transformer may operate at operating points with lower power efficiencies than at the nominal or rated (maximum) efficiency during a typical load cycle.

The type of operation, configuration, selection of materials, cooling system, and insulation of a transformer determine economic factors. It has been known for more than 100 years that electricity generation, transmission, distribution, and consumption are best done with three-phase and not with single-phase systems: the investment cost per installed power unit is smallest for three-phase systems. This applies to transformers as well: three single-phase transformers can be assembled to one three-phase unit and a considerable amount of raw materials can be saved, because the flux within the common-core portion is zero ($\phi_{\text{total}} \equiv 0$) for balanced operation ($\phi_{\text{Amax}} = \phi_{\text{Bmax}} = \phi_{\text{Cmax}}$) on account of the trigonometric identity $\phi_{\text{Amax}} \cos \phi + \phi_{\text{Bmax}} \cos (\phi - 120^\circ) + \phi_{C\text{max}} \cos (\phi - 240^\circ) \equiv 0$, as shown in Fig. 1(b). Of course, it might be desirable from a repair and reliability point of view to employ three single-phase units instead of one three-phase transformer. Then repair can be performed on one single-phase rather than the entire three-phase transformer.

The selection of the cooling system is important. Depending upon the application, different types of liquid cooling systems can be employed, ranging from oil-immersed self-cooled transformers to oil-immersed,

forced-oil-cooled transformers with pumps and fans and water coolers. A considerable amount of cooling liquid is required. A 1000 kVA transformer, for example, may hold from 1500 to 3500 L of oil, depending on its voltage rating. For a 1000 kVA transformer at a primary voltage of 4160 V, the oil adds approximately 1 ton to the total weight. This results in long (e.g., 4 h) thermal time constants of liquid-filled units.

Non-liquid-filled (dry-type) transformers are simpler in their construction—they consist of a core and windings, and mostly have no hermetically sealed tanks or eddy-current screens. This makes them less expensive than liquid-filled units, but their overload capacity is very small ($< 10\%$).

The selection of the insulation in transformers is important because insulation breakdown causes most transformer failures. Overheating is the predominant failure mode and leads to the premature aging of insulation materials. Lightning, overvoltages, low-level harmonic amplitudes of voltages and currents, and the employment of semiconductor converter loads producing transient voltage spikes contribute to insulation failure as well. The insulation of coils must be such that the electric field stress between the winding turns is nearly uniform. This calls for reinforced insulation near the terminals of a transformer, and control of the electric field stress along the lengths of winding turns.

Any device should be manufactured to perform its proper functions at minimum cost. The capabilities [overvoltage and overcurrent, total harmonic content (distortion) of voltages (THD_y) and currents (THD_i), short-circuit current, maximum temperatures, overload] of a transformer are limited; one can designate such performance characteristic data as inequality constraints. For example, the temperature θ of a transformer must be below a certain bound, $\theta \leq \theta_{\max}$. The minimum operating costs include initial investment, maintenance, storage costs, and the cost of transformer loss.

Transformer magnetic design is based on Maxwell's equations, and in particular Ampere's and Faraday's laws. The overall intent in the design of the magnetic circuit of a transformer is to minimize the air (butt-to-butt) gap lengths within the laminated transformer core (7). This reduces the excitation-current requirement for setting up the flux within the core. Hand calculations based on the two above-mentioned laws and numerical calculations (the so-called finite-element and finite-difference methods, *FEM* and *FDM*, respectively) are frequently applied. These numerical methods have been developed during the past 30 years and are very useful for design and performance optimization of transformers. In liquid-filled units, oriented (anisotropic) electrical steel laminations are predominantly employed. This permits maximum flux densities up to $B_{\max} = 2.5$ T within the core. Tests for the determination of transformer parameters—for example, impedances and short-circuit ratio, noise level and motion of windings, and insulation properties—are the (1) open-circuit and short-circuit tests, (2) sound level and vibration test, and (3) overvoltage test (2, 4), respectively.

Besides off-line monitoring of transformer characteristics, on-line monitoring of the integrity of a transformer is important. Such monitoring schemes record at any instant the temperature at different locations and materials of a transformer (e.g., winding, iron core, coolant) and the gas development in oil-immersed transformers due to low-level discharge currents caused by arcing of emerging short circuits (7). These monitoring techniques provide input for the protection of transformers. Transformers are the most delicate components within the transmission system, and their protection is important. All units, therefore, have overcurrent, differential-current, and overvoltage protection circuits.

Primary and secondary overcurrent relay circuits disconnect the transformer in case there are currents larger than the rated currents. If the overcurrent is small, the relay disconnects only if this current exists over a long period of time. The larger the overcurrent is, the shorter the time after which the inverse relay characteristic initiates the separation of the transformer from either the system or the load.

The differential-current relay compares the input current with the output current and initiates disconnection if the primary magnetomotive force (*mmf*)—defined as the primary instantaneous current times the primary number of turns—sufficiently differs from the secondary mmf. Similar considerations apply to overvoltage relays. Overvoltages up to 110% of the rated voltage can be tolerated for a certain amount of time.

A rather new development relates to the quality of power: monitoring transformers under nonsinusoidal conditions gives a measure of derating. Depending upon the current and voltage harmonic distortion, acceptable

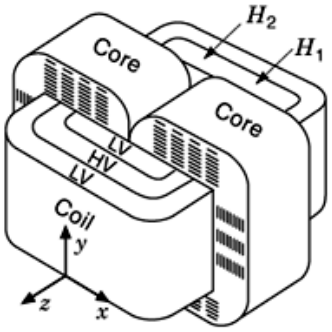

Fig. 2. Shell-form single-phase transformer. A ring winding is wrapped around two wound cores.

apparent power derating values range from 0 to 20%, as will be discussed later. Monitoring circuits measure iron-core, winding, and total losses online while the transformer operates on the system. The nonlinear load of the transformer can therefore be adjusted so that the total losses do not exceed the rated losses.

This technique is used for monitoring the impacts on transformers of geomagnetic storms due to sunspot cycles. It is known that the plasmas of solar eruptions influence the earth's magnetic field and these changes induce low-frequency (a few hertz) currents within transmission lines built on igneous rock formations (e.g., in the Rocky Mountain region). Such low-frequency currents and their resulting magnetic fields within high-voltage transformers result in additional reactive power demands, causing the terminal voltages to drop, and inducing collapse of the power system. Circuits for measuring asymmetric $(\lambda–i)$ characteristics of three-phase transformers and the zero-sequence $(\lambda_0–i_0)$ characteristic are presented in this article. Results show that parameters (e.g., currents, voltages, reactances, losses) of the above events in asymmetric three-phase transformers with three limbs can be accurately measured, simulated, and predicted.

This article concludes with a brief discussion of the state of the art of superconducting transformers.

Engineering Design

The engineering design of transformers is based on two constructions (2): the shell form (Fig. 2) and the core form [Fig. 1(a)]. The shell form consists of interleaved primary (e.g., HV in Fig. 2) and secondary (e.g., LV in Fig. 2) windings formed into a single ring, where HV and LV stand for high voltage and low voltage, respectively. Oriented magnetic steel laminations are assembled to form two cores encircling each side of the ring winding of Fig. 2. The mean length of a winding turn of the shell-form unit is usually larger than that of a comparable core-form unit, while the average iron core length is shorter for the shell-form than for the core-form unit. The core-form construction consists of anisotropic magnetic steel laminations arranged to provide a single-path magnetic circuit. Primary and secondary windings are grouped together on each main or vertical limb of the core. The shell form is predominantly used for low power ratings, while the core form is used for large units, especially for three-phase configurations. In the design of a particular transformer, many factors such as insulation and mechanical stress, heat distribution, weight, and cost must be balanced.

A three-phase power transformer for different voltages and currents can be constructed either by interconnecting three single-phase units to form a three-phase transformer bank [Fig. 1(b)], or by designing a three-phase unit [Fig. 1(c)]. The inherently asymmetric three-phase unit has the advantage of greater efficiency, smaller size, and less cost than a bank having equal apparent power. In a bank, however, it is possible to purchase and install a fourth unit at the same location as an emergency spare. This requires only 33%

additional investment to provide replacement capacity, whereas 100% additional cost would be required to provide complete spare capacity for a three-phase unit.

Three-limb, three-phase transformers are magnetically asymmetric and have a small zero-sequence reactance X_0 due to the large air gap between core and tank. Five-limb, three-phase units and symmetric three-phase banks have large zero-sequence reactances; this limits their use to applications where the large X_0 is not important. Detailed analyses can be performed with the method of symmetrical components, where forward (f), backward (b) and zero (0) sequence components are employed to investigate asymmetrical operating conditions of transformers such as line-to-ground and line-to-line faults.

Iron Cores

Oriented (anisotropic) silicon-steel laminations. The iron cores of conventional transformers consist of anisotropic silicon-steel laminations with lamination thickness ranging from 0.1 mm to 0.4 mm. In a transformer, the flux travels mostly within the limbs in the with-grain direction, and in the cross-grain direction only near the corners and lamination joints of transformer cores; thus oriented steel sheets are used. The with- and cross-grain structure of oriented steel is determined by the rolling direction of the sheets during manufacture. Each side of a lamination is coated with insulating material so that no eddy currents can flow between laminations. The coating does not significantly interfere with the passage of flux. The magnetic resistance, or *reluctance*, is only slightly increased and is taken into account via the iron-core stacking factor $\varphi_{\mathrm{Fe}} = \Sigma$(iron cross section of all laminations of core)/(cross section of entire core including insulation between laminations). The stacking factor is in the range of $0.93 \leq \varphi_{\mathrm{Fe}} \leq 0.97$ for 60 Hz units. Figure 3(a–c) illustrate the different types of cores based on oriented (anisotropic) steel sheets: the butt core, the wound core, and the mitered core (7). For anisotropic electrical silicon steel the relative permeability is larger (and thus the magnetization required is smaller) in the with-grain direction (direction of rolling) than in the cross-grain direction. Similarly, the core losses are small in the with-grain direction and relatively large in the cross-grain direction, as illustrated by Fig. 4 (8).

Amorphous (glass-type) cores. Amorphous magnetic materials either are obtained by quenching the molten material at high cooling rates or are manufactured by deposition techniques in a vacuum. The quenching process does not permit the forming of a crystalline structure, and therefore amorphous magnetic materials have a structure similar to glass. The cores of transformers with amorphous alloy (*AMT*s) can be fabricated in the same manner as those made of oriented-silicon-steel laminations [Fig. 3(a–c)]. METGLAS (trademark of the Allied Signal Co) cores are 30% heavier than comparable oriented silicon-steel cores, but the no-load losses in amorphous alloy wound cores (9) are only 30% of those in comparable oriented-silicon-steel wound cores. However, the rated power efficiencies of present-day designs of AMTs and silicon-steel pole transformers with wound cores are about the same. For example, the rated power efficiencies of 20 kVA and 50 kVA wound-core AMTs at unity power factor are $\eta_{\mathrm{power}} = 98.26\%$ and 98.59%, respectively, while that of a 25 kVA oriented-silicon-steel wound core (10) at unity power factor is $\eta_{\mathrm{power}} = 98.31\%$. The fabrication cost for AMTs with wound cores is higher than that for oriented-silicon-steel wound cores.

Primary and Secondary Windings

Primary and secondary windings of transformers can be manufactured either of copper or of less expensive aluminum wires or sheets. While the primary winding is connected to the source, the secondary winding is feeding the load; either winding can be the high-voltage or the low-voltage winding, depending on the type of transformer (step-up or step-down). Due to the ideal transformer relations $N_{\mathrm{p}}/N_{\mathrm{s}} = V_{\mathrm{p}}/V_{\mathrm{s}}$, the number of primary turns, N_{p}, is larger than the number of secondary turns, N_{s}, if the primary voltage V_{p} is higher

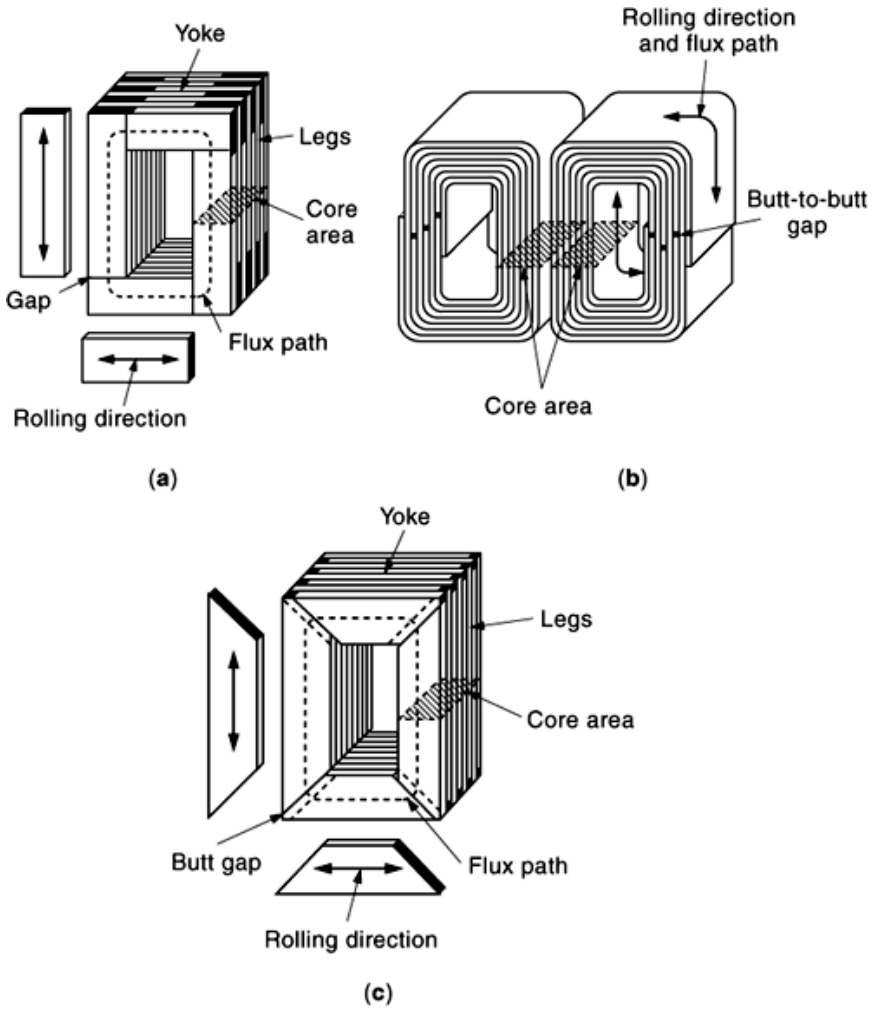

Fig. 3. Typical iron-core assemblies for either shell-form or core-form transformers: (a) butt, (b) wound, and (c) mitered cores.

than the secondary voltage V_s. By the same reasoning, since $N_pI_p = N_sI_s$ and $V_pI_p = V_sI_s$), the conductor cross section of the high-voltage winding is small and that of the low-voltage winding large. Fabrication and economic reasons dictate that the high-voltage (*HV*) winding is made of copper and sometimes the low-voltage (*LV*) winding is made of aluminum sheets, as shown in Fig. 5 (10). It is very difficult to manufacture thin aluminum wires reliably, while aluminum sheets can be manufactured easily; in addition, aluminum sheets are less expensive, but have a larger resistance, than comparable copper sheets.

Power and Energy Efficiencies

The nominal power efficiency η_{power} of a transformer is the ratio of rated real power output to rated real power input: $\eta_{power} = P_{out}/P_{in} = 1 - (P_{loss}/P_{in})$. Total losses P_{loss} are the sum of the no-load and load losses. No-load

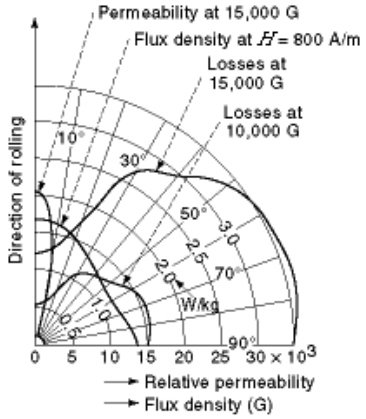

Fig. 4. Dependence of the relative permeability of oriented (anisotropic) electrical silicon steel laminations on the direction of the magnetic flux with respect to the grain orientation (rolling direction).

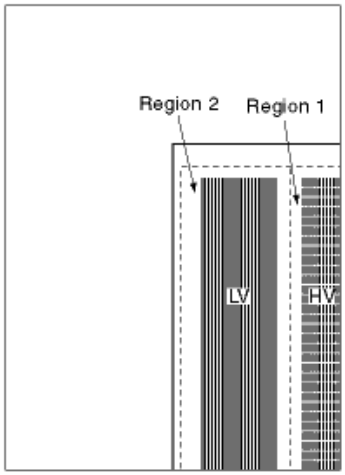

Fig. 5. Winding arrangement of one eighth of an $S = 25$ kVA oil-cooled, single-phase pole transformer. LV indicates the low-voltage winding consisting (in this case) of aluminum sheets, and HV the high-voltage copper winding.

losses consist of eddy-current and hysteresis losses within the core ($|\tilde{i}_c|^2 R_c$, the loss caused by the core-loss component i_c of the exciting current i_ϕ; see Figs. 7, 8 below), ohmic loss $|\tilde{i}_\phi|^2 R_p$, and dielectric loss: that is, all losses that occur at full voltage with the secondary circuit open. Load losses are $|\tilde{i}_p(t)|^2 R_p + |\tilde{i}_s(t)|^2 R_s$ caused by the primary $[i_p(t)]$ and secondary $[i_s(t)]$ load currents. Eddy-current losses also occur, induced by stray fluxes within the solid transformer structure, and similar losses are generated in the windings, varying with the load current. No-load losses are measured at rated frequency and rated secondary voltage (if the secondary side is the low-voltage side) and are considered to be independent of load. Load losses are measured at rated frequency and rated secondary current, but with the secondary short-circuited and with reduced voltage applied to the primary, the high-voltage side. Load losses can be assumed to vary as the square of the load current (2). Most units are not fully loaded all the time, and therefore one defines the energy efficiency of a transformer, where lightly loaded periods are also taken into account during a load cycle.

For low-power-efficiency transformers ($\eta_{power} < 96\%$) the loss can be measured from the relatively large difference between the input power P_{in} and the output power P_{out}. However, for high power efficiency units ($\eta_{power} > 96\%$), the errors in measuring P_{in} and P_{out} and the small difference between the two make an efficiency determination meaningless. If two current transformers (*CT*s, maximum errors $\varepsilon_{CT1} = \varepsilon_{CT2} = 5$ mA, CT ratio = 20) and two potential transformers (PTs, $\varepsilon_{PT1} = \varepsilon_{PT2} = 0.24$ V, PT ratio = 30) as well as two ammeters ($\varepsilon_{A1} = \varepsilon_{A2} = 5$ mA) and voltmeters ($\varepsilon_{V1} = \varepsilon_{V2} = 0.3$ V) with full-scale errors of 0.1% are used, then the maximum error in the measured losses for a 25 kVA, $\eta_{power} = 98.44\%$, 240 V/7200 V single-phase transformer at $\cos \phi_1 = 1$ is $\Delta P_{loss} = (240\text{ V} \pm \varepsilon_{PT1} \pm \varepsilon_{V1})(5.20835\text{ A} \pm \varepsilon_{CT1} \pm \varepsilon_{A1}) \times 20 - 30\ (240\text{ V} \pm \varepsilon_{PT2} \pm \varepsilon_{V2})(3.472\text{ A} \pm \varepsilon_{CT2} \pm \varepsilon_{A2}) = (240.54\text{ V}) \times (104.367\text{ A}) - (7183.8\text{ V}) \times (3.462\text{ A}) = 234.1$ W, so that $\Delta P_{loss}/P_{loss} = \pm (234.1/390)100\% \approx 60\%$. This means the conventional method of measuring the losses and therefore the power efficiency of high-efficiency units does not produce accurate results, and other methods must be used as described in a later section.

Technical–Economic Factors

Classification, type of operation, configuration, operating constraints. Many different types of transformers are available on the market today. Manufacturers' catalogs list them according to their ratings and construction features. They are often classified according to service or application, purpose, method of cooling, number of phases, types of insulation, and methods of mounting. There are single-phase pole transformers (e.g., 25 kVA to 50 kVA, 120 V_{ph} – 240 V_{ph}/ 7.2 kV_{ph}), three-phase substation transformers (e.g., 300 kVA to 500 kVA, 13.2 kV_{l-l}/138 kV_{l-l}), three-phase transmission units (e.g., 10 MV to 100 MV, 138 kV_{l-l}/380 kV_{l-l}), and three-phase transformers for extrahigh-voltage systems (e.g., 300 MV to 800 MV, 380 kV_{l-l}/765 kV_{l-l}). Note that for single-phase transformers the phase (ph) voltages are given, and for three-phase units the line-to-line (l–l) voltages.

Some transformers serve as a filter, blocking triple current harmonics, and must have an appropriate configuration, such as tertiary windings. Others must be insensitive to geomagnetically induced currents and thus require three-limb core transformers instead of a three-phase bank or a five-limb core unit: that is, the zero-sequence reactance (inductance) must be small enough to suppress zero-sequence fluxes and currents, requiring a large effective gap between tank and core, such as is possible for three-limb units. Transformers serving nonsinusoidal loads must be derated, and if they supply three-phase rectifiers of low harmonic distortion they must convert 3-phase (6-pulse) to 6-phase (12-pulse) or to 12-phase (24-pulse) systems. Recent developments with respect to six-phase generation and transmission require transformers with Δ and Y windings on the primary and secondary, respectively. Units used to adjust voltage and reactive power flow must be equipped with winding taps. High-efficiency and high-power units are equipped with either copper or high-permeability screens, reducing the magnetic field within the tank and thus minimizing tank losses.

The installation requirements of liquid-filled transformers are more stringent than those of dry-type units: due to their flammable coolants (e.g., mineral oil), transformers must be in a concrete vault if installed indoors and must have a flue to remove combustible gases; the total apparent power must in this case not exceed 112.5 kVA. The maximum ambient temperature must be 40°C, and units should operate below an altitude of 1000 m. For higher ambient temperatures and altitudes, transformers must be derated.

Selection of windings, core, and insulation. Efficiency considerations may require a certain selection of winding and core materials such as copper windings and laminated (oriented) silicon steel wound cores. In the latter the flux travels mostly along the with-grain direction, and therefore the iron-core losses are fairly small, but larger than those of wound amorphous cores. The core loss increase due to mechanical stress of wound cores is relatively small (8, 11).

The output power of any transformer is primarily limited by the winding temperature rise, more specifically by the absolute hot-spot temperature. According to the National Electrical Manufacturers Association

(*NEMA*), the allowable hot-spot temperature depends on the type of insulation as described by the letters O, A, B, F, H, and C, corresponding to 90°C, 105°C, 130°C, 155°C, 180°C, and 220°C, respectively. According to Ref. 1 the insulation is described as class 90, 105, 120, 150, 185, 220, or over 220, where the numbers represent the maximum allowable temperature in degrees Celsius.

Most liquid-filled transformers utilize class B insulation, corresponding to a limiting (hot-spot) absolute temperature of 130°C. At this temperature the pressurized mineral oil, which serves the double purpose of cooling and insulating the windings, does not yet boil. Bubbles form in an oil-filled transformer at a hot-spot temperature of around 140°C, releasing various gases from the oil. Thermal decomposition of cellulose also takes place.

Transformers supplying power to solid-state converters must have improved insulation, due to the exposure to parasitic high-frequency transient voltages and currents. The insulation class of a transformer is determined by the dielectric tests that the unit can withstand, rather than by the rated operating voltage. On a particular system, the insulation class of the connected power transformers may be determined from the ratings and characteristics of the protective devices installed to limit surge voltages across transformer windings. Ratings of the protective devices will in turn depend upon the type of system, its grounding connections, and other related factors. Excessive temperature rise is the primary cause of insulation failure (12, 13).

The low-voltage windings are located close to the core and consist of multilayer helical coils with cooling ducts between layers. The high-voltage windings are subdivided into a number of individual coils of a few turns per layer stacked one above the other and connected in series. In this way the interlayer potential stress is greatly reduced. The high-voltage windings are then assembled concentrically over the low-voltage windings. Spacers are arranged radially between high- and low-voltage coils to form cooling ducts and keep both windings apart

Selection of cooling system. The selection of a cooling system based on liquids permits a greater overload capability. Liquid-filled units are cooled in a variety of ways. Some of them protect the coolant from oxidation by sealing the transformer and inserting inert gas in the air space (7), as shown in Fig. 6. The following types of liquid-cooled transformers are the most common ones (2, 14, 15).

(1) *Oil-Immersed Self-Cooled* The insulating mineral oil circulates by natural convection within the tank, which has either smooth sides, corrugated sides, integral tubular sides, or detachable radiators.
(2) *Oil-immersed self-cooled and forced-air cooled* The same as type 1, but the addition of fans increases the rate of heat transfer from the cooling surfaces, thereby increasing the permissible transformer output.
(3) *Oil-Immersed Self-Cooled and Forced-Oil–Forced-Air Cooled* The rating of an oil-immersed transformer may be further increased by the addition of some combinations of fans and oil pumps.
(4) *Oil-Immersed Forced-Oil-Cooled with Forced-Air Cooler* Heat transfer from oil to air is accomplished in external oil-to-air heat exchangers with oil pumps and fans.
(5) *Oil-Immersed Water-Cooled* Cooling water runs through pipes that are in contact with the cooling oil of the transformer. The oil flows around the outside of these pipe coils by natural convection, thereby effecting the desired heat transfer to the cooling water.
(6) *Oil-Immersed Forced-Oil-Cooled with Forced-Water Cooler* External oil-to-water heat exchangers are used in this type of unit to transfer heat from oil to cooling water.

Depending upon the geometric duct dimensions and the pressure applied by the oil pumps, the oil velocities for laminar flow range from 0.005 m/s to 0.05 m/s. A great disadvantage of mineral oil is its flammability. For this reason nonflammable synthetic oils were developed, such as those with the brand names Askarel, Inerteen, Pyranol (USA), Permitol (England), Aroclor (France), and Clophen (Germany). Unfortunately, most of these have proven to be undesirable from an environmental and health point of view, and are not used in new transformer designs.

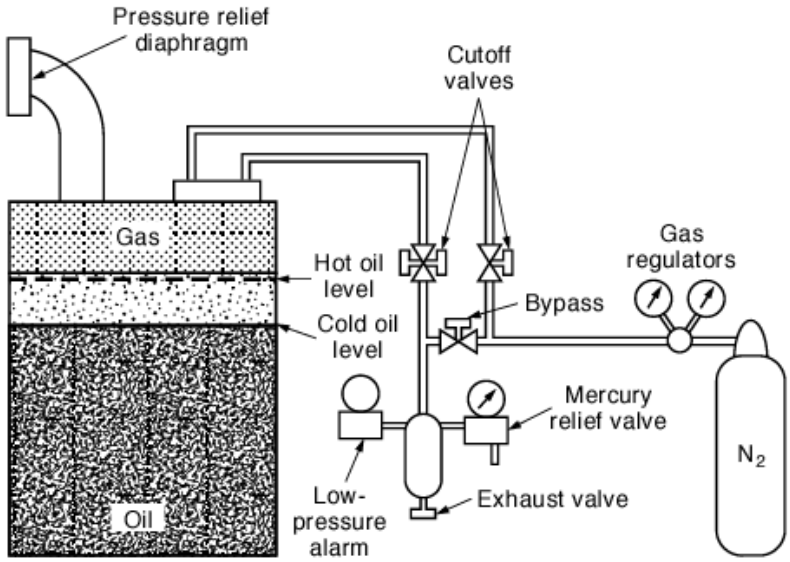

Fig. 6. Gas-sealed power transformer (7). The core and the windings are submerged in mineral oil, which expands due to temperature rise. Nitrogen gas prevents the oil from absorbing moisture and permits its expansion, resulting in varying pressure within the rigid tank.

Optimization of Transformer Efficiency Characteristic

Most transformers within the power system are not always operated at the rated load point, and thus optimal operation must take into account that the load on the transformer changes over the life of the unit and is dependent on the load growth. The load on a distribution transformer is very cyclic in nature, and as a result the transformer only operates at its maximum efficiency for very short periods of time. The cycle is simultaneously daily and yearly, with the peak load only existing for three or four hours per day. Therefore, energy efficiency plays an important role. Common methods of economic analysis for loss evaluation techniques are as follows (16):

(1) *Present worth of annual revenue requirements*, which is the proper method of evaluating economic alternatives in load growth situations.
(2) *Total levelized annual cost.* This method is equivalent to the present worth of annual revenue requirements under conditions of load growth, but no inflation.
(3) *Annual cost* leads to the same result as equivalent investment cost (or capitalized cost) when load growth is not considered.
(4) For the *equivalent investment cost* approach, it is necessary to divide the energy cost component of losses by the carrying finance charge rate. This converts the energy cost from an annual cost ($/kW·y) to an investment cost ($/kW), which can then be added directly to the demand cost component of losses and the transformer cost. Conversely, for the annual-cost approach it is necessary to multiply the demand cost component of losses and the transformer cost by the carrying finance charge rate. This converts these costs from an investment cost to an annual cost, which can then be added directly to the energy-cost component of losses to obtain a total annual cost.

The losses in a (distribution) transformer are real power losses, reactive power losses, and voltage regulation losses (drops).

In summary:

(1) Such a loss evaluation should aid in choosing between existing designs of different loss levels and initial costs.
(2) For a given set of input parameters there is an optimum set of load and no-load losses that will minimize the total levelized annual cost of a transformer.
(3) It is possible to include in the optimization the amount of energy that is required to produce the raw materials for transformers. In order to manufacture a more efficient unit, more materials must be used. To decrease load losses, more aluminum and/or copper must be employed in the windings; in order to decrease no-load losses, more iron in the core and/or more turns in the windings must be used. These materials have a certain energy content—that is, energy is required to manufacture the materials. Generally, less energy is associated with low-loss designs, despite the fact that more energy is required to manufacture such designs. Therefore, from a total-energy standpoint, it is worth using the extra energy to manufacture a more efficient transformer.

Magnetic Design

Equivalent circuit and phasor diagram. A more complete theory of transformer performance than that based on the ideal-transformer approach must take into account the effects of winding resistances (R_p, R_s), magnetic leakage, and fringing fluxes, as well as the excitation current $i_\phi(t)$. Sometimes the capacitances of windings—particularly for high-frequency operation (kilohertz to megahertz)—and transient phenomena such as lightning strikes must be taken into account.

The total flux linking the primary winding $\phi_p(t)$ can be divided into two components: (1) the resultant mutual flux $\phi_m(t)$ confined essentially to the iron core, and (2) the primary leakage flux $\phi_{lp}(t)$, which links only the primary. Because the leakage path is largely in air, the leakage flux and the voltage induced by it vary linearly with the primary current $i_p(t)$. In addition, there will be a voltage drop in the primary winding effective resistance R_p. The impressed terminal voltage $v_p(t)$ is then opposed by three voltages: the $i_p(t)R_p$ drop, the $L_{lp}di_p/dt$ drop, and $e_p(t) = \omega f N_p \phi_{max} \cos \omega t$ induced by the resultant mutual flux $\phi_m(t) = \phi_{max} \sin \omega t$. The resultant mutual flux $\phi_m(t)$ links both the primary and secondary windings and is created by their combined magnetomotive force (mmf): $N_p i_p - N_s i_s$.

The primary mmf $N_p i_p$ must meet two requirements of the magnetic circuit: it must (1) counteract the demagnetizing effect ($-N_s i_s$) of the secondary circuit current i_s, and (2) produce sufficient mmf ($|N_p i_p| > |N_s i_s|$, or $N_p i_p - N_s i_s \geq 0$) to create the resultant mutual flux $\phi_m(t)$. According to this physical picture, it is convenient to resolve the primary current into two components: a load component $i_s'(t)$ (the prime means referred to the primary) and an excitation component $i_\phi(t)$. The load component $i_s'(t)$ is defined as the component current in the primary that would exactly counteract the mmf due to the secondary current $i_s(t)$, that is, $N_p\, i_s'(t) = N_s\, i_s(t)$, or $i_s'(t) = N_s i_s(t)/N_p$ (see Fig. 7). The exciting current can be resolved into a core-loss current $i_c(t)$ in phase with $e_p(t)$ and a magnetizing component $i_m(t)$ lagging $e_p(t)$ by 90°. In general, the core-loss resistance $R_c = 1/G_c$ and the lossless magnetizing reactance $X_m = 1/B_m$ are nonlinear and depend upon the maximum flux densities within the iron core (8, 17). Note that B_m is a susceptance. Provided one assumes the T equivalent circuit of Fig. 7, the phasor diagram (Fig. 8) can be drawn for sinusoidal quantities. In Figs. 7 and 8 a tilde indicates complex quantities (phasors).

Numerical methods. Knowing the equivalent air gap length g_{equiv} within the iron core and the exciting mmf, the flux $\phi_m(t)$ can be calculated from Ohm's magnetic law $\phi_m(t) = \text{mmf}/R_{equiv}$, where the reluctance R_{equiv}

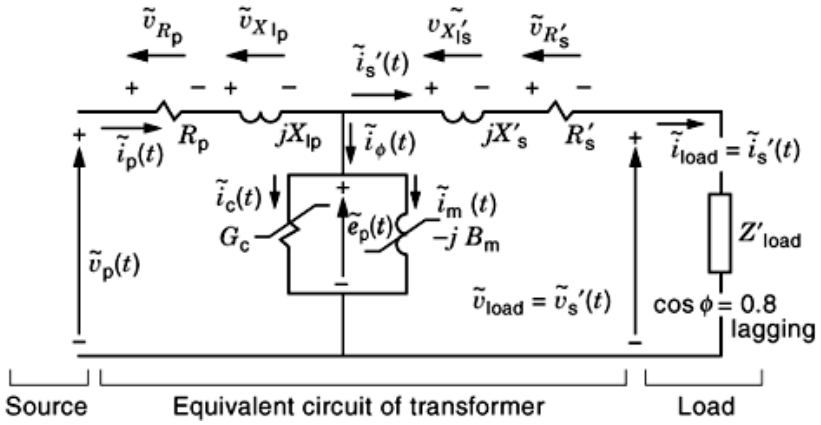

Fig. 7. T equivalent circuit of two-winding transformer including series and excitation branches. The conductance G_c and the susceptance B_m are assumed to be nonlinear. All other parameters are considered to be linear. A tilde represents complex quantities (phasors).

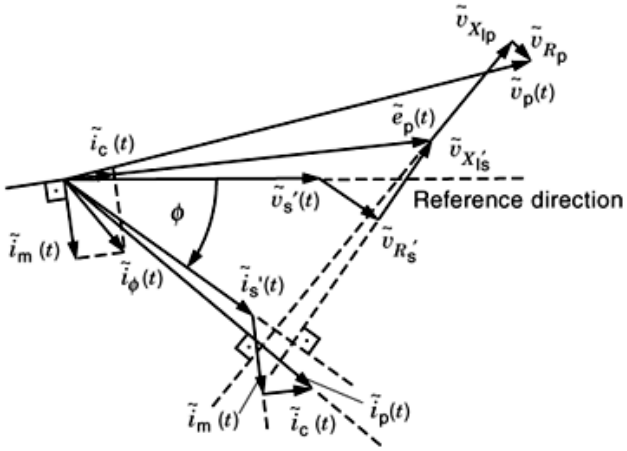

Fig. 8. Phasor diagram of two-winding transformer as it is derived from Fig. 7. A tilde represents complex quantities (phasors).

is a function of g_{equiv}. The problem associated with hand calculations is the uncertainty of the equivalent gap length g_{equiv} and the treatment of the nonlinear, anisotropic, multivalued B–H characteristics of the core. During the past 30 years numerical methods such as the FDM and FEM (11, 18) have found widespread application. They solve, for nonlinear anisotropic B–H characteristics, Poisson's partial differential equation in rectangular coordinates (x, y, z), subject to Dirichlet and Neumann boundary conditions, for the vector potential component A_z, current density J_z, and reluctivity ν:

$$\frac{\partial}{\partial x}\left(\nu\frac{\partial A_z}{\partial x}\right) + \frac{\partial}{\partial y}\left(\nu\frac{\partial A_z}{\partial y}\right) = -J_z \qquad (1)$$

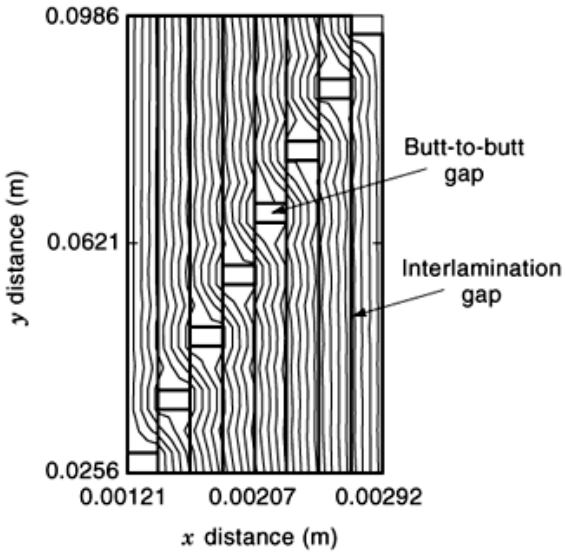

Fig. 9. Sample strip for mixed cross-grain and with-grain region for the calculation of a representative *B–H* characteristic. Flux does not cross the butt-to-butt gaps, but crosses instead the interlamination gaps, minimizing the equivalent reluctance of the laminated (wound) core.

The variational problem equivalent to solving Poisson's equation (1) is that of minimizing the energy-related functional

$$F = \iint_{\text{region } R(x,y)} \left(\int_0^B \nu b \, db \right) dx \, dy - \iint_{\text{region } R(x,y)} \left(\int_0^{A_z} J_z \, da_z \right) dx \, dy \qquad (2)$$

where b and B are flux densities, a_z and A_z vector potentials, J_z the current density, and ν the reluctivity. Both methods generate the same results (18) for the same discretization of the transformer geometry and for the same solution algorithm of the resulting (non)linear equation system.

Figure 9 illustrates the flux distribution for the nonlinear, anisotropic overlap joint core design of a shell-type transformer (7, 18,19,20,21). Although most flux travels in the with-grain direction, the flux passing through the mixed-grain limb (region with the overlap joints) of either core (Fig. 2) must briefly (due to butt-to-butt gaps) travel cross-grain and cross the interlamination gaps (8, 11, 17, 19). For this reason a representative *B–H* characteristic must be developed to describe the electrical steel in the outside limb of either core section (Fig. 2). A rectangular grid structure (8, 11) is used to approximate these outside limbs and to calculate this representative *B–H* characteristic. The sample strip consists of eight laminations with butt-to-butt and interlamination gaps to simulate the overlap joint region of the core. The measured with-grain and cross-grain *B–H* characteristics as provided by the steel manufacturer and the computed representative *B–H* characteristic (11) are depicted in Fig. 10. A quasi-three-dimensional field analysis generates, for the grid structure in the *x–y* [Fig. 11(a)] and *y–z* planes, the magnetostatic fields of Fig. 11(b,c). An evaluation of these field plots leads to the calculated λ–i characteristic (Fig. 12), which is compared with the measured one; here λ is the flux linkage. The agreement between the two is excellent—even near the knee. Such a good agreement cannot be achieved without properly modeling the butt-to-butt gaps of Fig. 9 (8, 11).

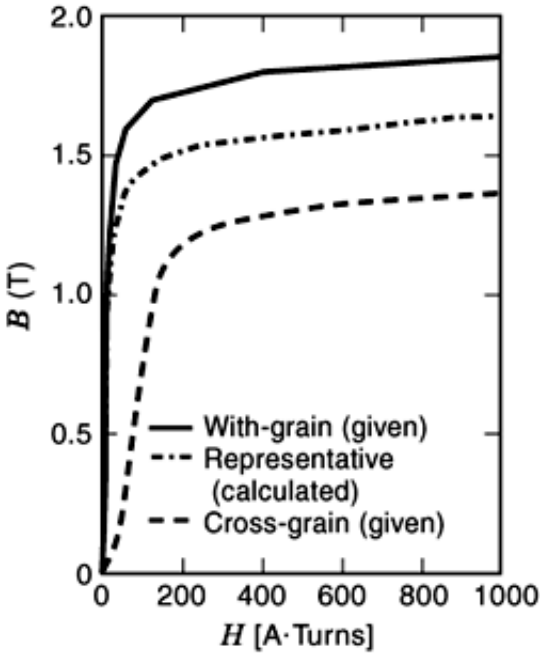

Fig. 10. Measured with- and cross-grain *B–H* characteristics and computed representative *B–H* characteristic of the sample strip of Fig. 9.

The calculation of the iron-core losses under nonsinusoidal conditions can be based on measured with-grain and cross-grain *B-loss functions*, calculated representative mixed-grain *B*-loss function as depicted in Fig. 13, and harmonic loss *phase factors* [Fig. 14(a,b)] (11, 19). The latter ones are measured with an Epstein frame by superposing the desired percentage of voltage harmonics on the fundamental and recording the change in losses compared to sinusoidal voltage. Voltage harmonics were superposed at phase angles of 0° and 180°, resulting in *peaky* (p–p of nonsinusoidal waveform is maximum) and *flat* (p–p of nonsinusoidal waveform is minimum) voltage waveforms, respectively. Experience has shown that these phase factors vary about linearly between these two extremes, and thus the phase factors for angles between 0° and 180° are found by linear interpolation (11, 19). These curves are the source of the alternating loss pattern for peaky and flat voltages of Fig. 15(a,b).

The calculation of the eddy-current losses in windings and cores requires the solution of the diffusion equation for nonlinear, anisotropic *B–H* characteristics and Dirichlet as well as Neumann boundary conditions (10), where $\tilde{A}_z$ denotes the complex vector potential:

$$\frac{\partial}{\partial x}\left(\nu\frac{\partial\tilde{A}_z}{\partial x}\right)+\frac{\partial}{\partial y}\left(\nu\frac{\partial\tilde{A}_z}{\partial y}\right)=-\tilde{J}_z+j\omega\sigma\tilde{A}_z \qquad (3)$$

To be able to compute eddy currents within individual turns, a very detailed grid structure for the primary and secondary windings must be used [Fig. 16(a,b)]. The solution of the above diffusion equation yields at $f_1 = 60$ Hz for the real and imaginary vector potentials under quasilinear (operating-point-dependent) conditions, as illustrated in Fig. 17(a,b). From these results the eddy currents can be calculated. The ac winding resistance R_{ac} as a function of the harmonic frequency f_h can be found, as shown in Fig. 18 for linear (unsaturated) and

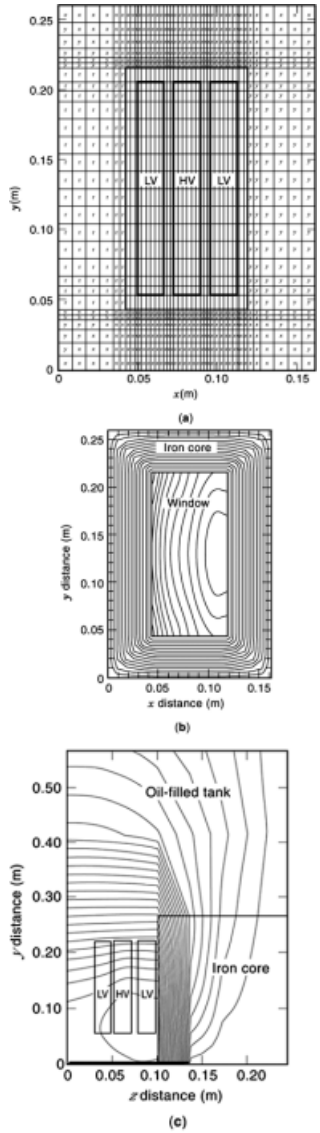

Fig. 11. (a) Grid structure for numerical field calculation in x–y plane of single-phase transformer. Grain directions are indicated by x and y. The overlap joints are identified by r. (b) Magneto-static flux distribution in x–y plane. The flux tubes within the window contain less flux than those within the core. (c) Magnetostatic flux distribution in y–z plane. Flux tubes do not contain equal flux.

nonlinear (saturated) cores (10, 22). R_{EC} (corresponding to the slope of the characteristics in Fig. 18) and the exponent ε of $(f_h/f_1)^{\varepsilon}$ can be determined from the numerical analysis indicated above. Knowing P_{EC-R} (p.u.) and the factors K (22) and F_{HL} (23), the derating of transformers can be computed under nonsinusoidal condition, as discussed in a later section.

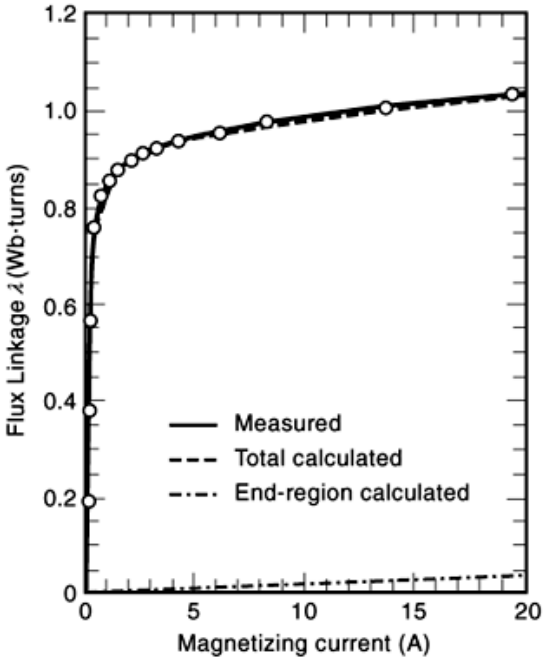

Fig. 12. Measured and calculated λ–i characteristics. The agreement between the two is excellent even near the knee.

Grounding, Protection, and Monitoring

Grounding and protection. According to the National Electric Code (*NEC*) (7), the purpose of grounding is threefold:

(1) To keep non-current-carrying metallic parts of transformers at zero potential of the earth to protect personnel who come in contact with them
(2) To limit excessive voltages caused by lightning, transients, and line faults
(3) To stabilize the voltage with respect to ground and facilitate the operation of overcurrent protection devices when a ground fault occurs

Closely related to grounding is the protection of units as mandated by NEC if electric faults occur. Transformers are designed for a particular voltage and maximum kilovoltampere rating. When these values are exceeded, the insulation quality is reduced, and serious damage or destruction can occur. Both overvoltages and excessive currents degrade the insulation quality. Overvoltages often exceed the dielectric strength of the insulation material, and arc-over occurs. Excessive currents cause the temperature of the transformer to exceed its rating. Therefore, the unit must be protected from both overvoltages and excessive currents. The most important protective devices are surge arresters, fuses and breakers, primary overcurrent relays, secondary overcurrent relays, differential current relays, and overvoltage relay, resulting in a completely self-protected (*CSP*) transformer. Underfrequency relays are sensitive to fractional (inter-, sub-, noninteger) harmonics (24) for amplitudes above 0.5%. Protection schemes specific to liquid-filled units include pressure valves, pressure relief diaphragms, low-pressure alarms, and nitrogen gas regulators.

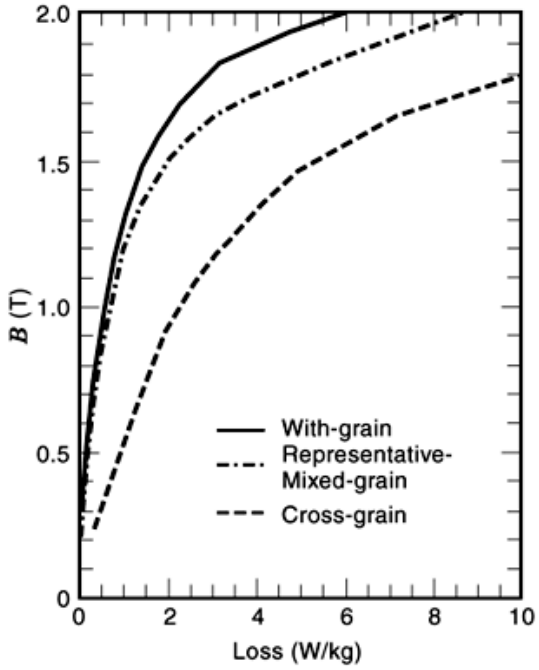

Fig. 13. Measured with- and cross-grain loss–*B* curves and calculated mixed-grain loss–*B* curve. These characteristics are required for the calculation of the iron-core losses.

While off-line monitoring (e.g., testing of coolant with respect to moisture content and dielectric properties, testing of insulation material, high-potential testing, short-circuit test, high-voltage dielectric test, and voltage and loss test) is presently much more common than on-line monitoring, the latter is becoming more important in predicting abnormalities as they develop during operation, so that they can be taken care of during scheduled outages. This minimizes the down time of a transformer.

Monitoring of temperature and noise. The on-line monitoring of temperature within the core, windings, and coolant is based on thermistors or thermocouples. Sound and vibration levels can be detected by acoustic and vibration sensors. Although liquid-filled units are predominantly installed far away from human contact—limiting acoustic noise levels to maxima in the range of 25 dB to 90 dB, if units are located within buildings or factories—such on-line measurements are useful to detect changes in the magnetic behavior of a transformer resulting from partial winding short circuits and deficient insulation properties.

Monitoring of gas development in oil-immersed distribution transformers. A gas analysis (14, 15) makes it possible to spot troubles before a failure occurs. For example, high-voltage arcing will cause ozone to form. Some coolants, when heated, give off gases that will ignite and explode. Coolants are combined chemically so that they do not give off enough explosive gases until their temperatures exceed 180°C. Only class H-rated transformers are designed to operate with winding temperatures this high (7).

New Developments

Derating of transformers. It is well known that voltage and current harmonics generate additional temperature rises that may lead to premature failures, and the rated lifetime (e.g., 40 years) of transformers

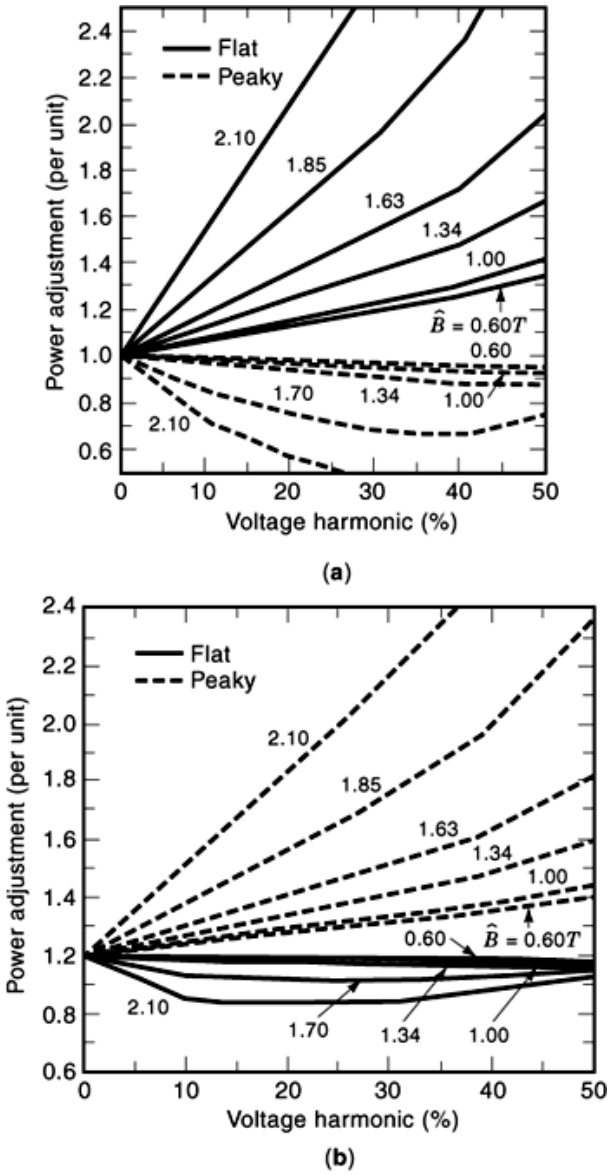

Fig. 14. Harmonic loss phase-factor curves for peaky and flat voltage waveforms due to (a) third and (b) fifth harmonics. These functions are useful for the calculation of the iron-core losses, which depend on the wave shape of the induced voltage (or the maximum flux density $\tilde{B}$ within the core).

may not be reached. To prevent such a failure the derating of a unit is designated such that the rated temperature rise is not being exceeded even when supplying nonsinusoidal load currents. Provided the cooling conditions are not altered, the rated temperature rise calls for a limitation of the losses under nonsinusoidal load identical to the rated losses occurring at linear load. The losses of a single-phase transformer can be

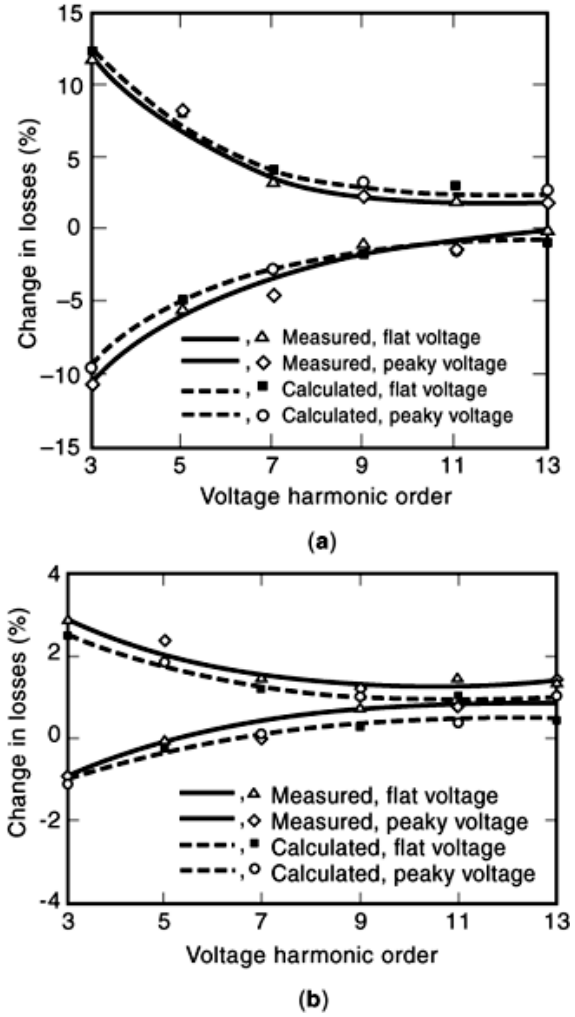

Fig. 15. Effect of 10% voltage harmonics on transformer losses at (a) no load and (b) full load. Note the alternating pattern of the change in losses as a function of the order of the harmonic voltage.

measured while operating under any load such that (8, 11, 19, 22, 23)

$$P_{\text{loss}} = \frac{1}{T}\int_0^T (v_{\text{p}} i_{\text{p}} - v_{\text{s}} i_{\text{s}})\, dt = \frac{1}{T}\int_0^T [v_{\text{p}}(i_{\text{p}} - i_{\text{s}}) + (v_{\text{p}} - v_{\text{s}}) i_s]\, dt \qquad (4)$$

As a result of this on-line measurement of the transformer losses one obtains, for example, Fig. 19(a) and Fig. 19(b), representing, respectively, the reduction in apparent power rating (*RAPR*) of a liquid-filled 25 kVA pole transformer and its real power capability (*RPC*) as functions of THD_i. Measured results agree with those of the well-known K (22) and F_{HL} (23) factors used to determine harmonic heating in transformer design. An application of this monitoring method to three-phase units is given in Fig. 20, where the total measured losses are expressed in terms of voltage and current differences [see Eq. (5)] that can be directly calibrated, and

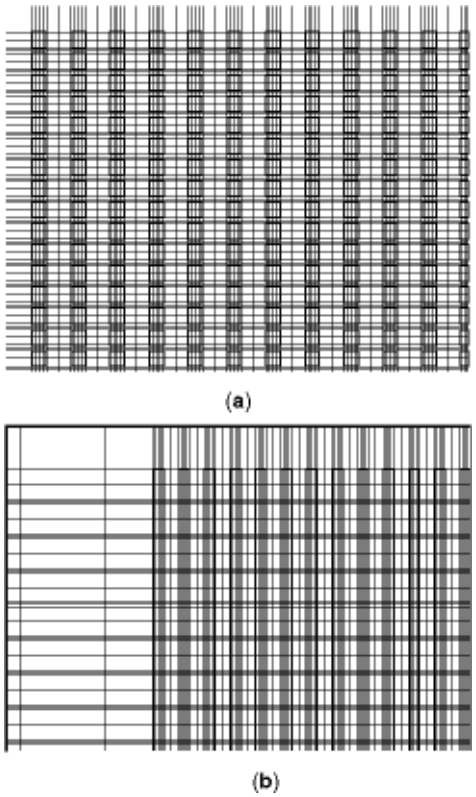

Fig. 16. (a) Partial grid structure of high-voltage winding (see region 1 of Fig. 5), and (b) partial grid structure of low-voltage winding (see region 2 of Fig. 5). In order to approximate the skin effect within copper conductors, each wire of region 1 must be represented by at least eight meshes. Similar considerations apply to the aluminum sheets of region 2 of Fig. 5.

therefore yield errors in the losses that are much smaller (e.g., less than 6 %) than those of the conventional method discussed in a prior section:

$$P_{\text{loss}} = \frac{1}{T}\int_0^T (v_{\text{AC}} i_{\text{A}} + v_{\text{BC}} i_{\text{B}} - v_{\text{ac}} i_{\text{a}} - v_{\text{bc}} i_{\text{b}})\, dt$$
$$= \frac{1}{T}\int_0^T [v_{\text{AC}}(i_{\text{A}} - i_{\text{a}}) + v_{\text{BC}}(i_{\text{B}} - i_{\text{b}}) + (v_{\text{AC}} - v_{\text{ac}}) i_{\text{a}} + (v_{\text{BC}} - v_{\text{bc}}) i_{\text{b}}]\, dt \tag{5}$$

Measurement of nonlinear λ–i characteristics. Three-phase transformers—in particular three-limb units—are magnetically asymmetric, and therefore the λ–i characteristics of all three legs are different. Figure 21 illustrates the circuit for measuring these nonlinear λ–i characteristics of limbs A and B (see Appendix F of Ref. 25). For measuring each limb's magnetic λ–i characteristic it is important to excite two phases of the three-phase winding and let two limbs have the same flux magnitudes in opposite directions (Fig. 21): that is, two phases of the low voltage windings are connected in parallel with reversed polarity. If the positive terminals of phases A and B are T_1 and T_2, respectively, and the negative terminals are T_4 and T_5, then T_1 and

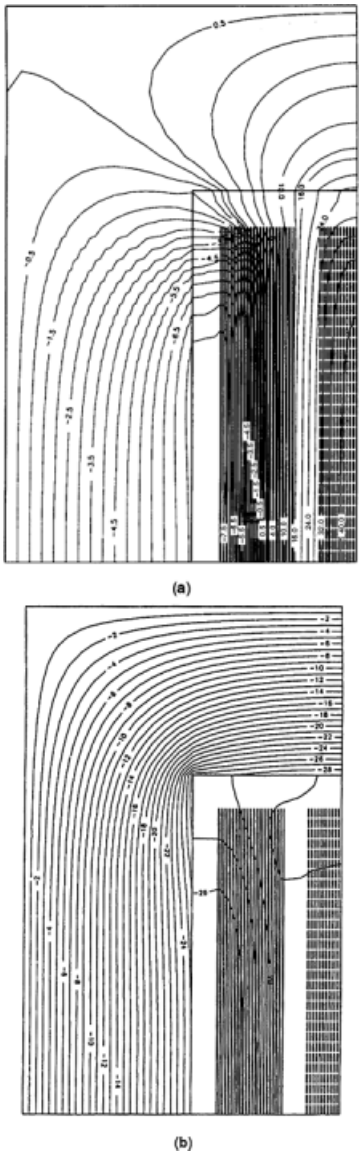

Fig. 17. (a) Real part and (b) imaginary part of vector potential $\tilde{A}_z$ if high-voltage (7.2 kV) winding is excited and low-voltage (240 V) winding is short-circuited at $f_1 = 60$ Hz. The bounding potentials for each flux tube are indicated.

T_5 are connected to the positive terminal of the voltage source and T_2 and T_4 to its negative terminal. From the magnetic circuit shown in Fig. 21 one notes that the flux passing through the third limb must be zero. For example, if phase C is not excited, ϕ_C is zero. For phases A and B one obtains (without tank)

$$F_A = i_A N_A = R_A \phi_A, \qquad F_B = i_B N_B = R_B \phi_B \tag{6}$$

where R_A and R_B are reluctances.

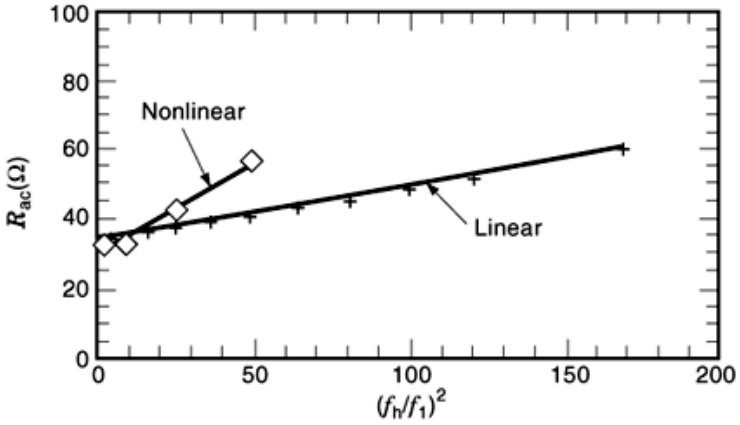

Fig. 18. Ac winding resistance R_{ac} as a function of the square of the frequency from dc to 780 Hz. The function labeled "Linear" is the result of measurements and calculations at (unsaturated iron core) short-circuit condition with low voltage and rated current. The function labeled "Nonlinear" is obtained at (saturated-iron-core) rated voltage and current.

The fluxes ϕ_A and ϕ_B can be calculated by integrating the induced voltages of the secondary windings of the two excited phases (A, B). Then the hysteresis loop of flux linkage versus ampere-turns can be constructed. Leakage fluxes exist for each winding, and there are different voltage drops caused by the different currents of the two phases across their leakage reactances, although the voltage applied to the two phase windings is the same. However, only a very small difference between the two limb fluxes exists: at rated voltage, the difference is less than one percent of the limb's flux, causing an insignificant error.

The measurement of the zero-sequence λ_0–i_0 characteristic (including tank) is illustrated in Fig. 22. Based on these measured functions, a simulation program (25) computes the no-load currents as shown in Fig. 23(a,b) for abc and acb phase sequences.

Operation with dc bias. The reactive power demand (25 26 27 28) of transformers with balanced dc bias is shown in Fig. 24 for a three-phase, three-limb 2.3 kVA unit as a function of I_{dc}. Note that for small gaps between core and tank (zero-sequence inductance L_0 large) the reactive power demand is considerable, while for large gaps (L_0 small) the reactive power increase is almost nonexistent. However, for unbalanced dc bias the reactive power demand is large regardless of the magnitude of L_0.

Application of new nonlinear transformer model. The new model of Ref. 25 can analyze loaded three-limb, three-phase transformers including the effect of the tank when dc bias exists. Although dc bias effects (e.g., due to unbalanced rectifier loads and sunspot cycles) are not so prominent at full or partial loads as at no load, such operating conditions (with dc bias) are important for studying the reactive power demand (25,26,27,28) of power systems. The difference between the model without load and with load lies in the secondary-side electric circuit equations and the mmf balance equations.

To make measurements simple, the primary side is assumed to be in Y_0 (grounded) connection, the secondary side is assumed to be in Δ connection, and the load is Y-connected. Now the Y-connected load is transformed into an equivalent Δ-connected load with the equations

$$Z_{ab} = (Z_a Z_b + Z_b Z_c + Z_c Z_a)/Z_c \tag{7a}$$

$$Z_{bc} = (Z_a Z_b + Z_b Z_c + Z_c Z_a)/Z_a \tag{7b}$$

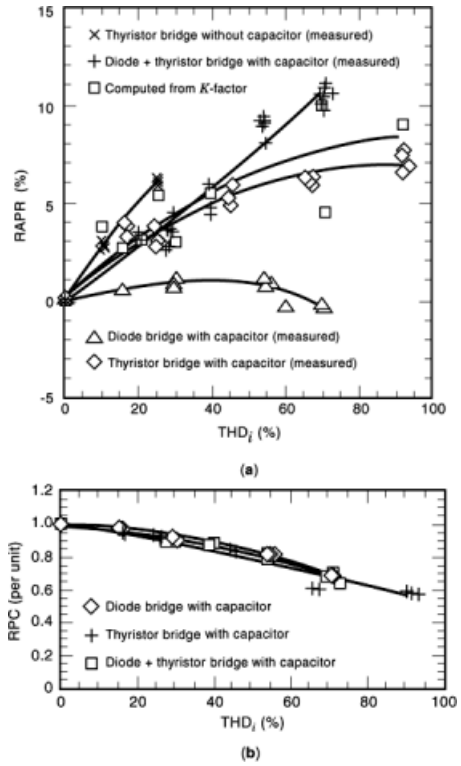

Fig. 19. (a) Reduction in apparent power rating (RAPR) of a 25 kVA, 120–240 V/7.2 kV oil-filled, single-phase transformer as a function of THD_i for different nonlinear loads. Note that thyristor loads result in the largest RAPR values. (b) Real power capability (RPC) of a 25 kVA, 120–240 V/7.2 kV oil-filled, single-phase transformer as a function of THD_i. For a given total harmonic current distortion of $THD_i = 95\%$, the reduction in *RPC* is much larger (e.g., 40%) than that in *RAPR* (e.g., 10%).

$$Z_{ca} = (Z_a Z_b + Z_b Z_c + Z_c Z_a)/Z_b \tag{7c}$$

The subscripts a, b, c refer to the low-voltage side, and A, B, C refer to the high-voltage side. Z_a, Z_b, Z_c are the load impedances of phases a, b, c, respectively, when they are Y-connected at the low-voltage side.

For the load side the following phasor equations are valid: First,

$$\check{I}_a + \check{I}_b + \check{I}_c = \frac{\tilde{E}_a + \tilde{E}_b + \tilde{E}_c}{Z_l} = 3\check{I}_0 \tag{8}$$

where Z_l is the leakage impedance of each phase (supposing the three windings have the same leakage impedance). In this particular equation Z_l corresponds to the zero-sequence impedance Z_0. Next,

$$\begin{aligned}&[Z_{ab}Z_{bc} + Z_{ab}Z_{ac} + \left(\sum Z_{ij}\right)Z_l](\check{I}_a - \check{I}_0) - Z_{ab}Z_{bc}(\check{I}_b - \check{I}_0) - Z_{ab}Z_{ca}(\check{I}_c - \check{I}_0)\\ &= \left(\sum Z_{ij}\right)\left(\tfrac{2}{3}\tilde{E}_a - \tfrac{1}{3}\tilde{E}_b - \tfrac{1}{3}\tilde{E}_c\right)\end{aligned} \tag{9}$$

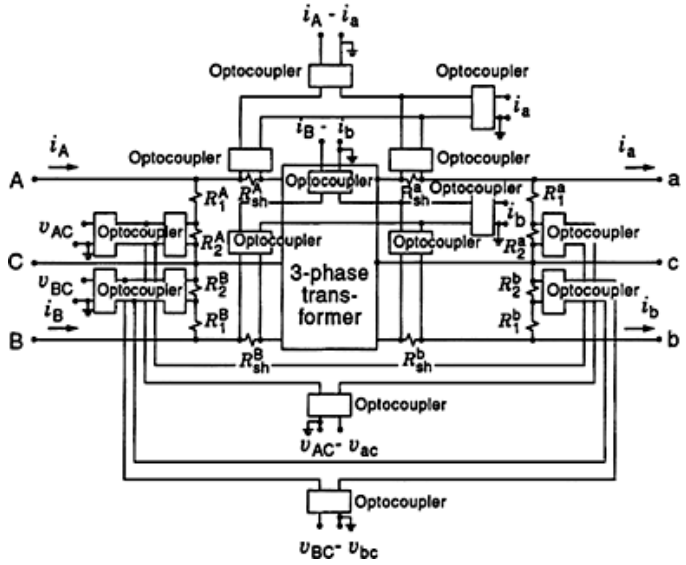

Fig. 20. Circuit for measurement of losses of a three-phase, three-wire transformer based on eight-channel data acquisition with analog-to-digital conversion. This circuit uses a new concept, where the losses of high-efficiency transformers ($\eta_{\text{power}} > 98\%$) are determined from current and voltage differences. These differences are directly calibrated, thus reducing the maximum error in the measured losses from about 60% (using the conventional method discussed in the section "Power and Energy Efficiencies") to about 6%. Iron-core and winding losses can be measured separately.

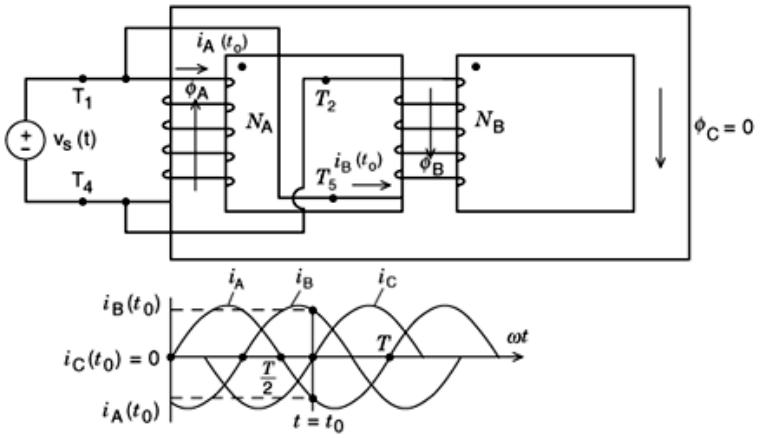

Fig. 21. Measurement circuit for nonlinear λ–i characteristics for limbs A and B. Asymmetric transformers [see Fig. 1(c)] can be modeled based on three different λ–i characteristics. This enables the calculation of asymmetric magnetizing currents.

$$-Z_{ab}Z_{bc}(\check{I}_a - \check{I}_0) + [Z_{ab}Z_{bc} + Z_{ca}Z_{bc} + \left(\sum Z_{ij}\right)Z_l](\check{I}_b - \check{I}_0) - Z_{bc}Z_{ca}(\check{I}_c - \check{I}_0)$$
$$= \left(\sum Z_{ij}\right)\left(\tfrac{2}{3}\check{E}_b - \tfrac{1}{3}\check{E}_a - \tfrac{1}{3}\check{E}_c\right) \qquad (10)$$

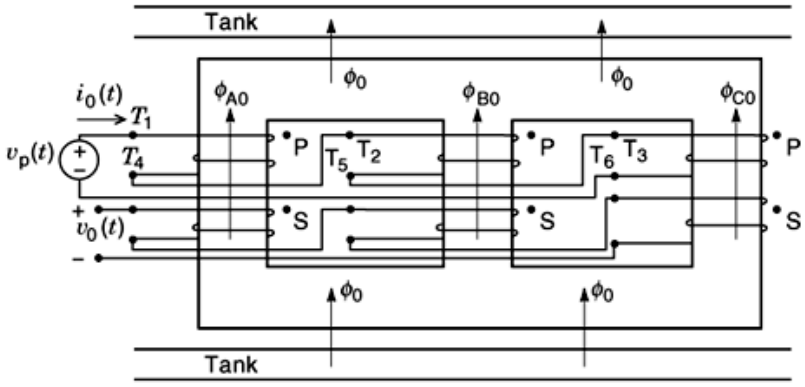

Fig. 22. Measurement circuit for zero-sequence λ_0–i_0 characteristic of a three-limb, three-phase transformer. This measurement circuit extends that of Fig. 21 and enables the modeling and computation of zero-sequence quantities.

where $\Sigma Z_{ij} = Z_{ab} + Z_{bc} + Z_{ca}$. If e_a, e_b, e_c, Z_{ab}, Z_{bc}, Z_{ca}, and Z_l (or Z_0) are given, then the secondary currents i_a, i_b, i_c, i_0 can be calculated by solving Eqs. (8) to (10) in the time domain. The voltages e_a, e_b, e_c are governed by the following relations:

$$N_a e_a = N_A e_A \tag{11}$$

$$N_b e_b = N_B e_B \tag{12}$$

$$N_c e_c = N_C e_C \tag{13}$$

and

$$\nu_A - \left(r_A i_A + L_{Al}\frac{di_A}{dt}\right) = e_A \tag{14}$$

$$\nu_B - \left(r_B i_B + L_{Bl}\frac{di_B}{dt}\right) = e_B \tag{15}$$

$$\nu_C - \left(r_C i_C + L_{Cl}\frac{di_C}{dt}\right) = e_C \tag{16}$$

$$R_A\phi_A - R_B\phi_B = N_A i_A - N_a i_a - (N_B i_B - N_b i_b) \tag{17}$$

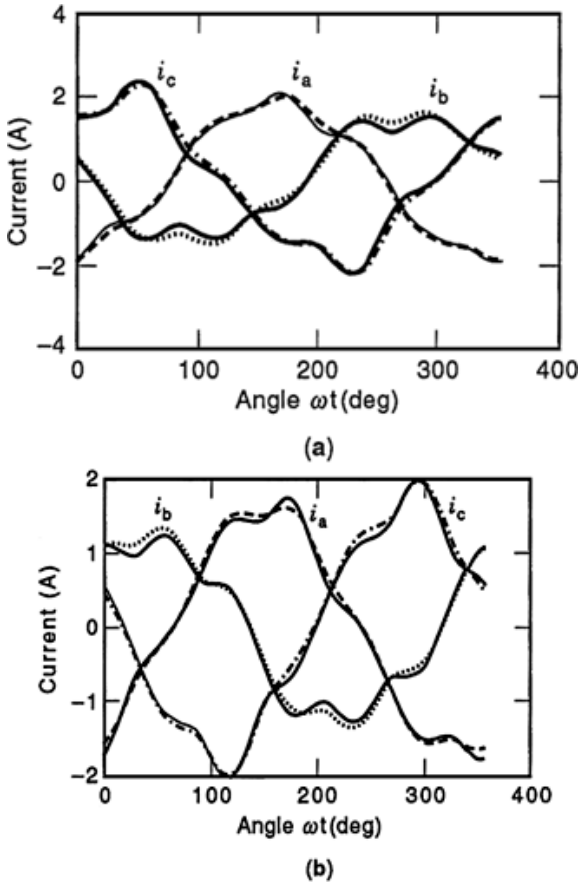

Fig. 23. Measured and computed no-load currents for asymmetric 2.3 kVA three-phase transformer (with three limbs) at rated voltage: (a) abc phase sequence, and (b) acb phase sequence. Measured: full lines; calculated: broken lines.

$$R_B\phi_B - R_C\phi_C = N_B i_B - N_b i_b - (N_C i_C - N_c i_c) \tag{18}$$

$$R_B\phi_B - R_0\phi_0 = N_B i_B - N_b i_b \tag{19}$$

together with Eqs. (1) to (13) of Ref. 27 and (6-1) to (6-5) of Ref. 25. The primary currents can be obtained by solving the above equations combining time-domain and frequency-domain methods as mentioned in Section 5.5 of Ref. 25.

Superconducting transformers. Low-temperature superconducting (*LTS*) transformers were first proposed in the 1970s, and designed to operate at 6°K to 14°K (−268°C to −260°C). The invention of high-temperature superconducting (*HTS*) materials increased the prospects for superconducting units designed to operate between 20°K to 77°K. A three-phase 630 kVA, 18.7 kV_{l--l}/420 V_{l--l} demonstration transformer based on HTS winding technology is presently under test on the power grid (29).

Superconducting transformers have about half the weight of conventional oil-filled transformers, and they require less space due to their reduced size, which is important for urban locations. They are nonflammable and

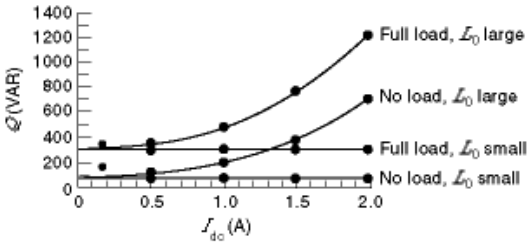

Fig. 24. Reactive power demand at various balanced dc biases for an asymmetric 2.3 kVA three-phase transformer (with three limbs). This analysis is important for the investigation of the effects of sunspot cycles on the operation of power systems. Similar phenomena occur in transformers, if unbalanced three-phase rectifiers generate dc components within three-phase transformers.

employ environmentally benign liquid nitrogen as the cooling medium. But perhaps the key advantage is their capability for overcapacity operation, due in part to the low temperatures at which HTS windings operate. Heat is the principal enemy of the paper-oil electrical insulation system of conventional power transformers. HTS transformers operate in the ultracold range of 20°K to 77°K (−253°C to −196°C), where insulation materials will not degrade. They can operate up to twice rated power, and they have a low series impedance, improving voltage regulation. Conventional transformers typically have $\eta_{\text{power}} = 99.3\%$ to 99.7% for the 30 MVA class. HTS transformers have a higher efficiency, to the extent that the reduced loss in a HTS unit can more than pay for its initial capital cost over its lifetime.

HTS units have a similar construction to the liquid-filled conventional transformer: the magnetic core carries superconducting windings cooled by liquid nitrogen, which is the only safe and low-cost cryogen available in liquid form in the 20°K to 77°K temperature range. The superconducting windings are manufactured either as wires or as flat tapes using BSCCO-2223 material. To date there are not many data available concerning the reliability of HTS units. Most publications concede that a superior, cost-effective HTS transformer technology might take two decades to become available.

BIBLIOGRAPHY

1. IEEE C57.12.80-1978 (R1992), *IEEE Standard Terminology for Power and Distribution Transformers (ANSI)*, New York: IEEE, 1978.
2. Central Station Engineers of the Westinghouse Electric Corporation, *Electrical Transmission and Distribution Reference Book*, 4th ed., Pittsburgh: Westinghouse, 1964.
3. IEEE C57.12.00-1993, *IEEE Standard General Requirements for Liquid-Immersed Distribution, Power, and Regulating Transformers (ANSI)*, New York: IEEE, 1993.
4. IEEE C57.12.90-1993, *IEEE Standard Test Code for Liquid-Immersed Distribution, Power, and Regulating Transformers and IEEE Guide for Short Circuit Testing of Distribution and Power Transformers*, New York: IEEE, 1993.
5. IEEE C57.91-1995, *IEEE Guide for Loading Mineral-Oil-Immersed Transformers (ANSI)*, New York: IEEE, 1995.
6. IEEE PC57.110/D7, *Recommended Practice for Establishing Transformer Capability When Supplying Nonsinusoidal Load Currents*, New York: IEEE, 1998.
7. G. P. Shultz *Transformers and Motors*, Indianapolis: Sams, 1989.
8. M. A. S. Masoum, Generation and propagation of harmonics in power system feeders containing nonlinear transformers and loads, Ph.D. Thesis, University of Colorado, Boulder, 1991.
9. S. Ezure *et al.* Long-term reliability of amorphous alloy wound core distribution transformers, *IEEE Trans. Power Deliv.*, **9** (1): 249–256, 1994.

10. T. Batan Real-time monitoring and calculation of the derating of single-phase transformers under (non)sinusoidal operation, Ph.D. Thesis, University of Colorado, Boulder, 1999.
11. T. D. Stensland Effects of voltage harmonics on single-phase transformers and induction machines including preprocessing for power flow, M.S. Thesis, University of Colorado, Boulder, 1995.
12. Y. C. Huang *et al.* Developing a new transformer fault diagnosis system through evolutionary fuzzy logic, *IEEE Trans. Power Deliv.*, **12** (2): 761–767, 1997.
13. T. K. Saha *et al.* Investigating the effects of oxidation and thermal degradation on electrical and chemical properties of power transformer insulation, *IEEE Trans. Power Deliv.*, **14** (4): 1359–1367, 1999.
14. H. T. Yang C. C. Liao Adaptive fuzzy diagnosis system for dissolved gas analysis of power transformers, *IEEE Trans. Power Deliv.*, **14** (4): 1342–1350, 1999.
15. J. Jalbert R. Gilbert Decomposition of transformer oils: a new approach for the determination of dissolved gases, *IEEE Trans. Power Deliv.*, **12** (2): 754–760, 1997.
16. Westinghouse Electric Corporation, *Optimization of Distribution Transformer Efficiency Characteristic*, Final Report DOE/RA/3022-01, Washington DC: US Department of Energy, 1980.
17. E. F. Fuchs M. A. S. Masoum D. J. Roesler Large signal nonlinear model of anisotropic transformers for nonsinusoidal operation, Parts I, II, *IEEE Trans. Power Deliv.*, **6** (1): 174–186, **6** (4): 1509–1516, 1991.
18. E. F. Fuchs G. A. McNaughton Comparison of first-order finite difference and finite-element algorithms for the analysis of magnetic fields, parts I, II, *IEEE Trans. Power Appar. Syst.*, **101** (5): 1170–1201, 1982.
19. T. Stensland *et al.* Modeling of magnetizing and core-loss currents in single-phase transformers with voltage harmonics for use in power flow, *IEEE Trans. Power Deliv.*, **12** (2): 768–774, 1997.
20. G. F. Mechler R. S. Girgis Magnetic flux distributions in transformer core joints, *IEEE Trans. Power Deliv.*, PE-126PWRD-1999.
21. E. G. Tenyenhuis G. F. Mechler R. S. Girgis Flux distribution and core loss calculation for single-phase and five-limb three-phase transformer core designs, *IEEE Trans. Power Deliv.*, **15** (1): 204–209, 2000.
22. E. F. Fuchs D. Yildirim W. M. Grady Measurement of eddy-current loss coefficient P_{EC-R}, derating of single-phase transformers, and comparison with K-factor approach, *IEEE Trans. Power Deliv.*, **15** (1): 148–154, 2000.
23. D. Yildirim E. F. Fuchs Measured transformer derating and comparison with harmonic loss factor (F_{HL}) approach, *IEEE Trans. Power Deliv.*, **15** (1): 186–191, 2000.
24. J. F. Fuller E. F. Fuchs D. J. Roesler Influence of harmonics on power system distribution protection, *IEEE Trans. Power Deliv.*, **3** (2): 546–554, 1988.
25. E. F. Fuchs Y. You D. Lin *Development and Validation of GIC Transformer Models*, Final Report 19X-SK205V, Oak Ridge,: Martin Marietta Energy Systems, 1996.
26. B. W. McConnell *et al. Impact of Quasi-DC Currents on Three-Phase Distribution Transformer Installations*, Final Report ORNL/Sub/89-SE912/1, Oak Ridge: Oak Ridge National Laboratory, 1992.
27. E. F. Fuchs Y. You D. J. Roesler Modeling, simulation and their validation of three-phase transformers with three legs under dc bias, *IEEE Trans. Power Deliv.*, **14** (2): 443–449, 1999.
28. Y. You *et al.* Reactive power demand of transformers with dc bias, *IEEE Ind. Appl. Soc. Mag.*, **2** (4): 45–52, 1996.
29. S. P. Mehta N. Aversa M. S. Walker Transforming transformers, *IEEE Spectrum*, **34** (7): 43–49, 1997.

EWALD F. FUCHS
University of Colorado Boulder